Nanotubes Protruding from Poly(allylamine hydrochloride)-Graft-Pyrene Microcapsules

Zhipeng Wang,[†,‡] Helmuth Möhwald,[‡] and Changyou Gao[†,*]

[†]MOE Key Laboratory of Macromolecular Synthesis and Functionalization, Department of Polymer Science and Engineering, Zhejiang University, Hangzhou 310027, China, and [‡]Max Planck Institute of Colloids and Interfaces, Research Campus Golm, 14424 Potsdam, Germany

ABSTRACT Protrusion of one-dimensional nanotubes or nanorods from the poly(allylamine hydrochloride)-graft-pyrene (PAH-Py) microcapsules was discovered when the microcapsules were incubated in pH 0 and pH 2 solutions, respectively. Micelles assembled from deliberately synthesized PAH-Py polymers were also able to transform into one-dimensional structures, demonstrating the chemistry driven nature of the phenomenon. The one-dimensional nanotubes consisted of only 1-pyrenecarboxaldehyde with ordered $\pi-\pi$ stacking, and showed a helical structure and anisotropic property. The hydrolysis of Schiff base and its rate at different pH values (10 times slower at pH 0 than at pH 2) played a key role in determining the final nanostructures, and the linear PAH directed the regular building up process especially for the nanotubes. Hollow capsules budded with nanotubes or nanorods mimicking the cellular protrusion of filopodia were successfully prepared by tuning the incubation pH and time. These results and the proposed mechanism open new opportunities for design of novel micronanostructures and materials for nanoscience, and biological and other advanced technologies.

KEYWORDS: microcapsules · protrusion · nanotubes · Schiff base · hydrolysis

Hollow capsules, as a special category of colloidal structures, possess isolated space and controllable permeability and thereby find diverse applications in medicine and food sciences and cosmetics, *etc.*[1−5] So far wide varieties of hollow structures such as polymersomes,[6,7] multilayer capsules,[8−11] and hollow microspheres[12−14] have been developed. The structure and morphology of the capsules play a key role in determining the capsule properties and functions. In particular, smart capsules can change their structure and properties intelligently in response to various stimuli such as pH, ionic strength, temperature, light, and even redox potential.[15−18]

Most of the intelligence of the formed hollow structures results from controllable swelling and shrinking as well as explosion,[19] but less from shape transformation. The latter was realized only for vesicles and hollow silica spheres.[20−26] For instance, a budded hollow silica sphere could be constructed by kinetic self-assembly of silica precursors and continuously budding surfactant.[20] Block copolymers could form vesicles of a special morphology with protruding rods and porous spheres by an increase of polymer concentration and exchange of solvent.[21−23] More interestingly, giant hyperbranched polymer vesicles experienced shape transformations in analogy to cellular processes such as birth, budding, fusion, and fission.[24−26] Therefore, not only the transformation process of the hollow structures is of high interest, but also the underlying physicochemical mechanisms which may give a hint on the biological and natural processes.[27] However, shape transformations of hollow microcapsules (MCs) have rarely been observed so far.

In this paper, we report the first discovery of protrusion of one-dimensional nanotubes (1D-NTs) from poly(allylamine hydrochloride) (PAH)-graft-pyrene (Py) MCs (Figure 1a). The detail study reveals that the protrusion dynamics and structures depend on the incubation pH value, which influences the hydrolysis rate of Schiff base between PAH and Py (Figure 1b).

RESULTS AND DISCUSSION

This discovery originated from the development of a simple but versatile strategy for fabricating MCs.[28] In this process, an -NH_2 containing polyelectrolyte, PAH, was doped into $CaCO_3$ particles during mineralization, and further reacted with 1-pyrenecarboxaldehyde (Py-CHO) by Schiff base formation. Removal of the $CaCO_3$ template yielded hollow MCs composed of Py modified PAH (PAH-Py) (Figure 1a,b). Scanning electron microscopy (SEM) (Figure 1c) revealed that the as-prepared PAH-doped $CaCO_3$ particles were ellipsoids with an average diameter of 5.5 μm. They had a rough surface morphology with a lot of tiny pores (Figure 1c, inset), which facilitated diffusion of Py-CHO and thereby its reaction with

* Address correspondence to cygao@mail.hz.zj.cn.

Received for review February 1, 2011 and accepted April 11, 2011.

Published online April 11, 2011
10.1021/nn200413d

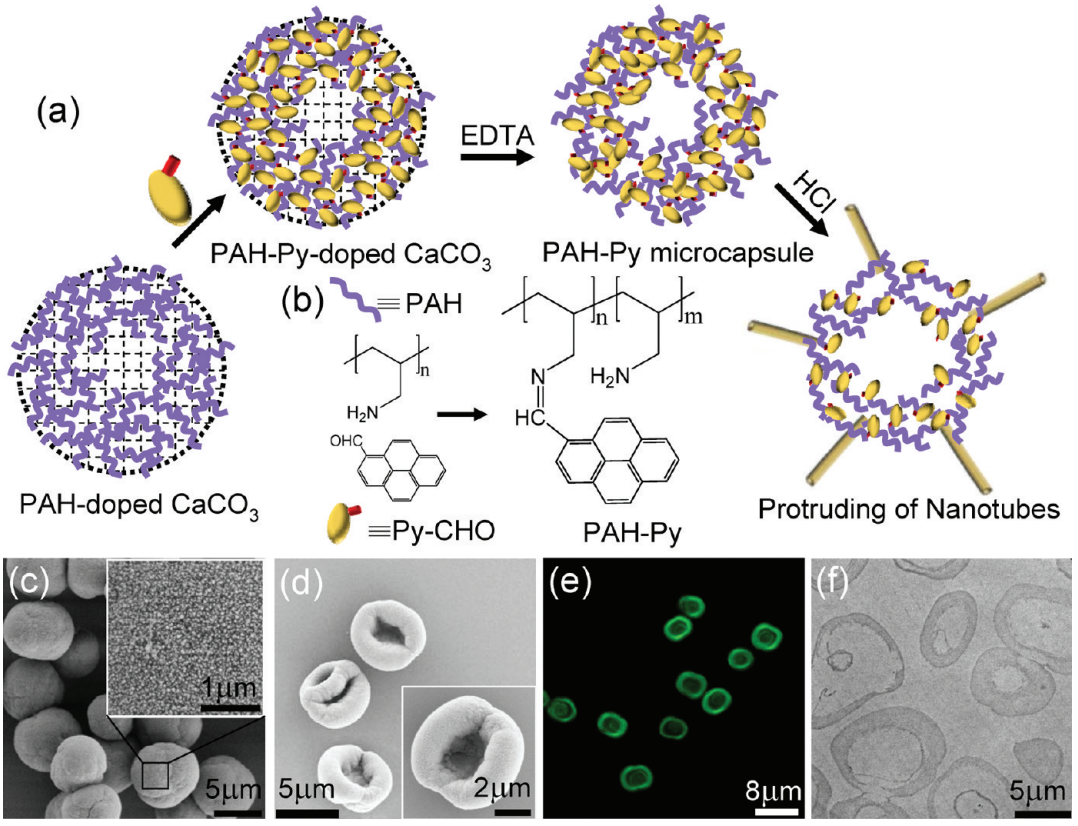

Figure 1. (a) Schematic illustration of PAH-Py microcapsule fabrication and 1D-NT protrusion. (b) Chemical structures of PAH, Py-CHO, and PAH-Py. (c) SEM images of PAH-doped $CaCO_3$ microparticles and their fine surface structure (inset). (d) SEM (inset, higher magnification). (e) Confocal laser scanning microscopy (CLSM) and (f) cross section (ultramicrotomy) TEM images of PAH-Py MCs.

PAH. By removing the sacrificial $CaCO_3$ with ethylenediaminetetraacetatic acid (EDTA) solution, MCs were obtained as a result of aggregation of the hydrophobic Py and rearrangement of the hydrophilic PAH chains (Figure 1d–f). Their size was identical with that of the template. The MCs collapsed only in the middle parts due to the very thick shells,[29] leading to a concave morphology (Figure 1d). FTIR spectroscopy (Supporting Information, Figure S1) identified the Schiff base bond at 1623 cm^{-1} in the PAH-Py MCs. No calcium was detected within the MCs by energy dispersive X-ray spectroscopy (EDX) (Figure S2). The fluorescent contour of the PAH-Py (Figure 1e) confirmed the thick capsule shell, whose thickness was 1.4 μm on average according to the MC cross section transmission electron microscopy (TEM) (Figure 1f). Elemental analysis reported a Py substitution degree of 19% on PAH in the MCs. By UV measurement using tetramethylrhodamine isothiocyanate labeled PAH, less than 5% of the original doped PAH (3% in $CaCO_3$ particles) was released from the MCs. This accounts for a shell thickness of 2.2 μm,[30] which matches well with the TEM data (1.4 μm). Previous results have shown that the PAH molecules reside in the periphery of the $CaCO_3$ particles as a result of additional physical adsorption of PAH on the porous and rough surface of the $CaCO_3$ particles,[28] and so does the PAH-Py distribution after the Schiff base reaction. Moreover, due to the osmotic pressure and outward flow during template removal, those PAH-Py molecules in the inner part also tend to accumulate to yield a dense peripheral PAH-Py layer. Therefore, thick hollow capsules instead of microspheres are obtained. Moreover, the stabilizing force within the capsules is the association between the hydrophobic domains of Py, which is unique, but applicable to other systems too.

Protrusion of the 1D-NTs was observed when the MCs were incubated in pH 0 HCl solution (Figure 2a–e). The original MCs appear dark without distinguishable fine structures (Figure 2a). After 24 hours, short and uniform 1D-NTs (~5 μm in length and <100 nm in width) start to grow from the MCs (Figure 2b). The 1D-NTs keep growing with incubation time (Figure 2c,d) and eventually form a network (Figure 2e). During this process, the MCs fade gradually (Figure 2d) and disappeared completely after 144 h (Figure 2e). If the process is terminated at an appropriate time such as 30 h by neutralizing the HCl, a MC budding with the NTs can be obtained (Figure 2f,g). The SEM image (Figure 2g) demonstrates that the NTs definitely grow from the MCs. When the incubation is terminated at 72 h, much thinner MCs with longer NTs are obtained (Figure 2h). Moreover, the incubation pH also has a big

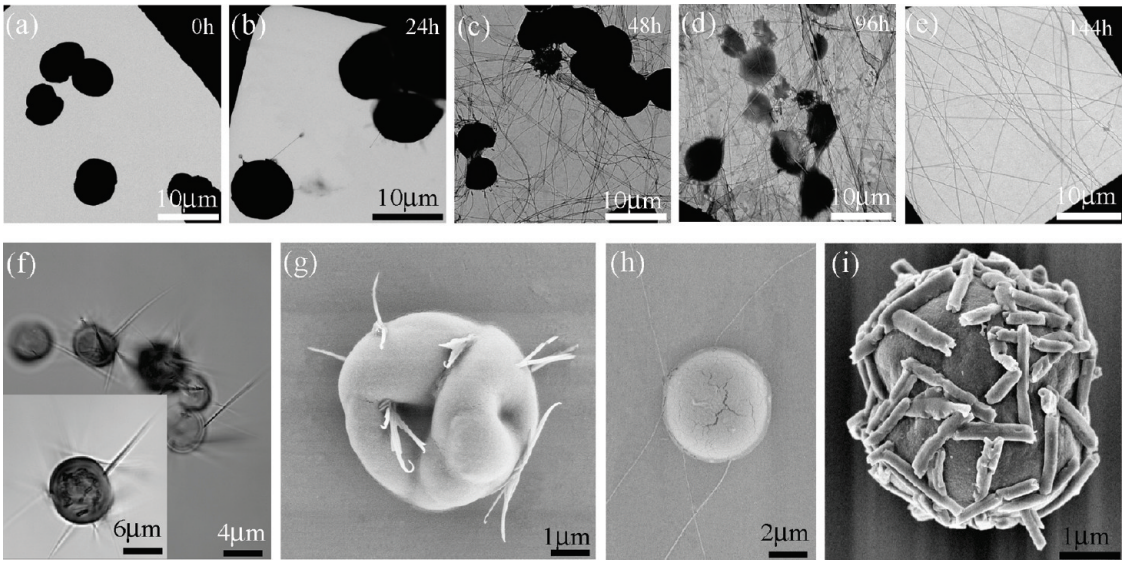

Figure 2. (a–e) TEM images showing the process of nanotube protruding from the PAH-Py microcapsules incubated in pH 0 HCl for 0, 24, 48, 96, and 144 h, respectively. (f) Optical images (inset, a higher magnification) showing the protruded nanotubes from the PAH-Py microcapsules incubated in pH 0 HCl for 30 h. SEM images of a microcapsule with nanotubes after treatment in pH 0 HCl for (g) 30 h and (h) 72 h, respectively. (i) SEM image of a microcapsule with nanorods after treatment in pH 2 HCl for 1 h.

impact on formation of the fine structures. For example, at pH 2 the MCs grow into short one-dimensional nanorods (1D-NRs) within 1 h instead of the long 1D-NTs, with a very fast transformation rate (Supporting Information, Figure S3). Again, termination of the incubation at 30 min resulted in MCs budded with a lot of short NRs (Figure 2i). These MC-NTs show a similar morphology as that of HEp-2 cells which have a lot of long and thin filopodia (Supporting Information, Figure S4), and thereby represent a brand new category of micronanostructures similar to the biological analogan.

Now that the capsule transformation is clearly identified, the question arises on the mechanism underlying this phenomenon. A preliminary characterization found that the 1D-NTs only consisted of Py-CHO with no PAH (Supporting Information, Figure S5). To facilitate the interpretation, PAH-Py polymers were synthesized in methanol solution and purified, which theoretically had the same chemical composition as the MCs except for the substitution degree. Special attention should be paid to the 1D-NTs formation, since their fibrillar hollow structure is more attractive.

The synthesized PAH-Py was characterized by ^{1}H NMR (Supporting Information, Figure S6). It had a substitution degree of 9.4%, which was the highest value achieved in solution synthesis. The Schiff base can be conjugated with the Py group to form a large π-system, which was clearly revealed by the shift of the Py excimer peak from 449 nm of Py-CHO to 508 nm of PAH-Py (Supporting Information, Figure S7).[31] The amphiphilic PAH-Py in water (pH 6.5) formed uniform micelles with an average diameter of 36 nm, as shown by TEM (Supporting Information, Figure S8). However, after treatment at pH 0 for 144 h the micelles were

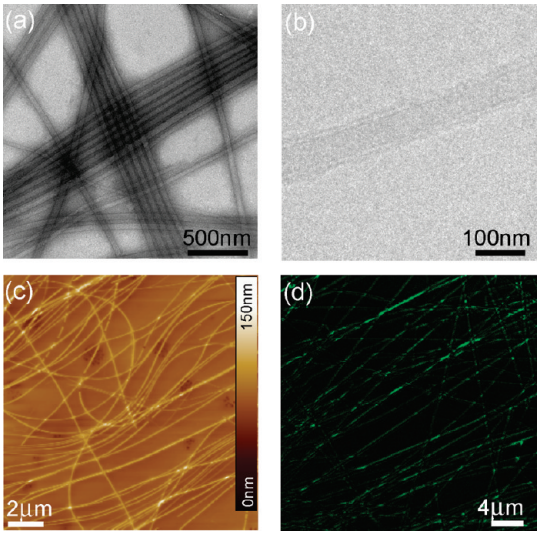

Figure 3. (a) TEM, (b) Cryo-TEM, (c) SFM, and (d) CLSM images of 1D-NTs prepared from PAH-Py polymers after incubation in pH 0 HCl for 144 h.

transformed to the 1D-NTs too, as confirmed by TEM (Figure 3a) and high magnification Cryogenic TEM (Cryo-TEM) image recorded in solution (Figure 3b). The tubes showed high uniformity in diameter (82 $\pm$ 16 nm by scanning force microscopy (SFM, Figure 3c)) and in wall thickness. Since the average height of the NTs in a dry state was only 19.1 nm (Figure 3c), some collapse must have happened to some extent. These 1D-NTs could be visualized by CLSM due to the presence of fluorophore Py molecules (Figure 3d). Therefore, formation of the 1D-NTs only depends on the chemical structure of the PAH-Py but not on its assembled 3D structures. In addition, the 1D-NRs could

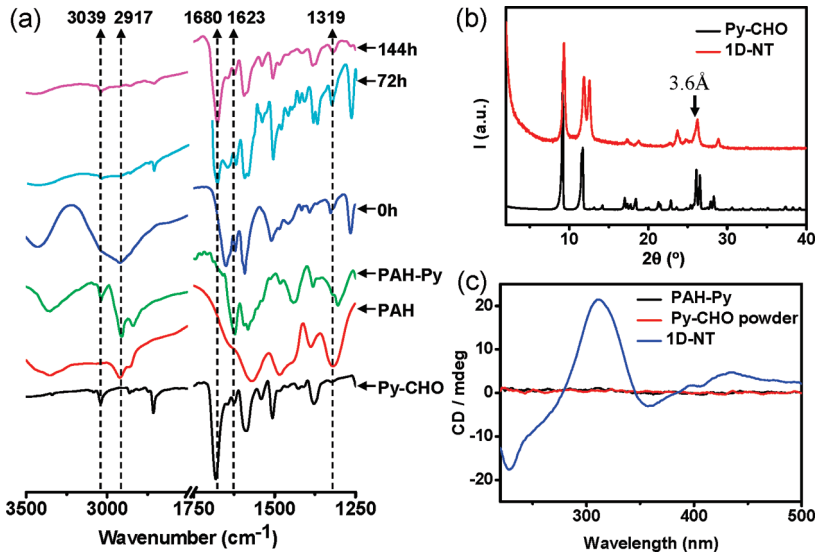

Figure 4. (a) Formation process of 1D-NTs monitored by FT-IR spectroscopy. Samples include Py-CHO, PAH, and PAH-Py (pH 6.5) as well as PAH-Py after treatment in pH 0 HCl solution for 0, 72, and 144 h, respectively. (b) XRD pattern of Py-CHO powder and 1D-NTs. (c) CD spectra of PAH-Py and 1D-NT solutions.

also be obtained within 1 h when the PAH-Py micelles were incubated in a pH 2 solution (Supporting Information, Figure S9), which is in accord with the case of PAH-Py MCs.

Formation of the 1D-NTs and/or 1D-NRs should exclusively depend on the change of the chemical structure of PAH-Py in response to a pH triggered hydrolysis of the Schiff base, as demonstrated by FTIR spectroscopy (Figure 4a). Again, the final 1D-NTs (144 h) were only composed of Py-CHO but not PAH as those obtained from the MCs (detailed description in Supporting Information). The X-ray diffraction (XRD) pattern of the 1D-NTs showed a sharp reflection at 2θ of 26.2° (Figure 4b), corresponding to a *d* spacing of 3.6 Å. This value matches well with the $\pi-\pi$ stacking distance between Py molecules in a crystal,[32,33] suggesting that the NTs are built up from the gradually disconnected Py-CHO *via* $\pi-\pi$ stacking. However, the crystal structure of the 1D-NTs was determined as monoclinic but not triclinic as for the Py-CHO powder (detailed crystal structure information in Supporting Information, Table S1), revealing that in the 1D-NTs the crystal symmetry is increased. A similar crystal structure was obtained for the NRs (Figure S10). Circular dichroism (CD) spectroscopy displayed positive (309 nm) and negative (352, 231 nm) signals for the 1D-NTs (Figure 4c), which are known as the Cotton effects for the $\pi-\pi^*$ transitions of Py-CHO.[34] However, no CD signals were recorded for the PAH-Py polymer and Py-CHO original powder. Therefore, the long-range orientational order should be only attributed to the special arrangement of Py-CHO in the 1D-NTs. Polarized optical microscopy showed that the $\pi-\pi$ stacking direction was parallel to the long axis of the NTs, confirming the anisotropy of the NTs (Supporting Information, Figure S11).[35] All the results suggest that the build up of the 1D-NTs from Py-CHO occurs in an ordered way and evolves gradually into larger dimensions. Therefore, the slow $\pi-\pi$ stacking of Py-CHO in solution is of key importance for the 1D-NTs formation.

Starting from the same material, PAH-Py, different nanostructures were obtained just by changing the pH. The control factor was found to be the hydrolysis rate of Schiff base which was monitored by UV−vis absorption spectroscopy. Taking the 1D-NT formation at pH 0 as an example (Figure 5a), the original PAH-Py solution showed a peak at 361 nm, which is similar to the absorption of the Py-CHO methanol solution and therefore assigned to Py-CHO. When the pH value was decreased to 0, the peak immediately red-shifted to 453 nm (red line), indicating that the Schiff base in the large π-system experienced protonation. During the 1D-NT formation, the absorption peak at 453 nm decreased gradually and disappeared after 120 h, whereas the original peak at 365 nm reappeared again. This alteration confirms the gradual hydrolysis of the Schiff base and formation of Py-CHO, which is in good agreement with the FTIR spectra (Figure 4a). A similar process happened in the 1D-NR formation at pH 2 (Figure 5b), which, however, was much faster than that at pH 0 and lasted only for 1 h.

To quantify the hydrolysis rate of Schiff base at different pH values, another experiment was designed (Figure 5c). During the Schiff base hydrolysis process, Py-CHO would disconnect from PAH and easily be extracted from water to toluene. Yet the Py on the hydrophilic PAH chain is hard to transfer to toluene. Thus, the Py-CHO content in toluene was quantified by UV−vis spectroscopy. It is proportional to the hydrolysis rate of Schiff base. According to Figure 5c, the hydrolysis rate of Schiff base in PAH-Py follows first-order kinetics at the beginning of the reaction.[36] Thus,

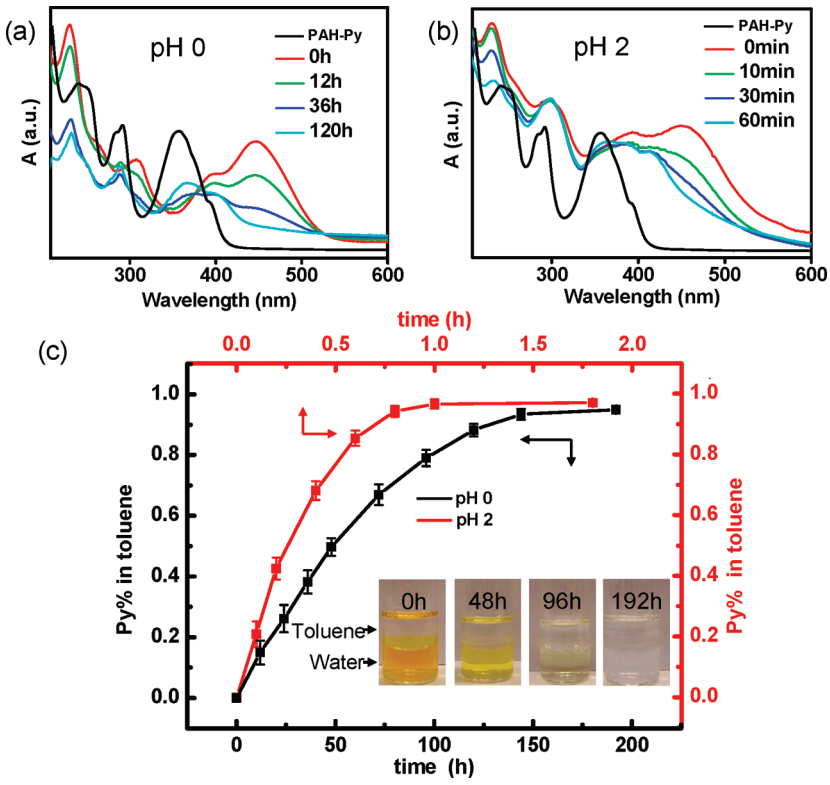

25

Figure 5. Formation process of 1D-NTs (a) and 1D-NRs (b) followed by UV–vis spectroscopy. (c) Quantitative comparison of the decomposition rate of the Schiff base in PAH-Py at pH 0 and pH 2. The Py-CHO content in toluene, which was extracted from water as shown in the inset pictures, increase with a different rate at different pH values.

the apparent hydrolysis rate constants (K_{obs}) were calculated to be 1.4×10^{-3} and 1.4×10^{-2} min^{-1} at pH 0 and pH 2, respectively. It is worth mentioning that the process of Schiff base decomposition and 1D-NT formation could even last more than 2 weeks at pH < 0. Moreover, these results are strongly supported by a previous kinetic research on the hydrolysis of the Schiff base, in which the hydrolysis rate decreases with increasing acidity (below pH 4).[36]

With a linear structure analogously to that of PAH, poly-L-lysine (PLL) could similarly direct the regular 1-D nanostructure formation (Supporting Information, Figure S12), but the branched polyethyleneimine (PEI) and small 1-butylamine could not (Figure S13). Moreover, when the Py-CHO was substituted by another hydrophobic ferrocene aldehyde, only amorphous precipitate was obtained. Therefore, formation of the nanostructures is controlled by all parts of the polyelectrolytes, the pendent groups, and the linking bonds between them.

Taking all the above results into consideration, the mechanism of protrusion of the nanostructures from the PAH-Py capsules is determined as follows. Incubation of the PAH-Py capsules in acid solution causes the protonation and hydrolysis of the Schiff base, which is significantly influenced by the pH value. At pH 0, the slow hydrolysis of Schiff base leads to long enough time for the pendent Py groups on the PAH chains to form partial $\pi-\pi$ stacks before they break up and further arrange in one dimension to form the 1D-NTs under the assistance of linear PAH chains. Indeed, it has been demonstrated that polyelectrolytes with regular repeat units such as PAH can function as template to assist the self-assembly process.[37] At pH 2, a large quantity of Py molecules become free in a very short time so that they aggregate due to their hydrophobicity in a more disordered way with less assistance of PAH, leading to the 1D-NRs formation. This is in accordance with the fact that the 1D-NRs exhibited no CD signals. It also explains the presence of both NTs and NRs in pH 1 solution (Supporting Information, Figure S14), in which the Schiff base has a moderate hydrolysis rate. Moreover, growth of the 1D-NTs and 1D-NRs follows a crystallization manner as well, starting from the crystal nuclei on the capsule walls and resulting in a continuous length increase.

CONCLUSION

Protrusion of 1D-NTs or 1D-NRs from the PAH-Py MCs was discovered when MCs were incubated in pH 0 and pH 2 solutions, respectively. The protrusion process of the nanostructures is triggered by pH and influenced by the incubation time, so that thickness of the MC shells and length of the NTs can be tuned to

form cellular-like hollow capsules budding with NTs or NRs. Deliberately synthesized PAH-Py polymers, which form micelles in solution, are also able to transform to the 1D-NTs and 1D-NRs, demonstrating that formation of the nanostructures depends only on chemical structure of the PAH-Py but not on its assembled 3D structures. The hydrolysis rate of Schiff base (10 times slower at pH 0 than at pH 2) at different pH plays a key role in determining the final physical structures, while the linear PAH directs the regular build up process especially for the NTs. The finding of 1D-nanostrucure protrusion from the PAH-Py MCs, the formed hollow capsules budded with NTs or NRs mimicking the cellular protrusion of filopodia, and the proposed mechanism open new opportunities for design of novel micronanostructures and materials for nanoscience, and biological and other advanced technologies.

EXPERIMENTAL SECTION

Materials. PAH ($M_n \approx 56$ kDa), Py-CHO, calcium nitrate tetrahydrate, sodium carbonate, and EDTA were purchased from Aldrich. HCl solution (1 mol/L) was purchased from Merck Company and diluted to the desired concentration. Other chemicals were used as received. The water used in all experiments was prepared *via* a Millipore Milli-Q purification system and had a resistivity higher than 18MΩ·cm.

Fabrication of PAH-Doped $CaCO_3$ Microparticles. PAH or TRITC-PAH was dissolved in 100 mL of 0.33 M calcium nitrate solution in a beaker under magnetic agitation (~600 rpm), into which an equal volume of 0.33 M sodium carbonate solution was rapidly poured at room temperature. The final PAH concentration was adjusted between 0.4 and 4 mg/mL. After 20 min, the PAH-doped $CaCO_3$ particles were centrifuged and washed for 3 times to get rid of the free PAH and salts.

Fabrication of PAH-Py Microcapsules. The as-prepared PAH-doped $CaCO_3$ microparticles were dispersed in ethanol and mixed with excess Py-CHO which was also dissolved in ethanol. After the mixture was kept in a vessel under mild agitation for 2 h, centrifugation and washing by ethanol were conducted several times until the excess Py-CHO was washed away. Finally, the Py-modified $CaCO_3$ microparticles were incubated in 0.2 M EDTA solution for 15 min under shaking to obtain the PAH-Py MCs, which were further washed with fresh EDTA solution and water, each for 3 times, using centrifugation (2000*g*, 3 min).

Fabrication of MC-NT Composites. The as-prepared PAH-Py MCs were incubated and dispersed in 1 M HCl solution under shaking. After a specified time, one portion of the solution was neutralized by 1 M NaOH solution, followed by gentle centrifugation and washing for 3 times. The whole transfer process from MC to NT lasted 5−6 days.

Synthesis of PAH-Py. To a solution of 0.6 g of potassium hydroxide in 6 mL of methanol 0.2 g of PAH (2.16 mmol repeat units) was added in small portions. The solution was stirred for 1 h at room temperature and then kept at 4 °C for 12 h. The precipitated potassium chloride was filtered off and the filtrate was dialyzed against methanol to completely get rid of the potassium hydroxide. Py-CHO (0.216 mmol, 50 mg) was dissolved in 5 mL of methanol and added to the dialyzed PAH methanol solution. The mixture was stirred for 30 min and then kept at 4 °C. The substituted polymers were collected by casting the methanol solution into 200 mL of acetone, followed by filtration. The Py substitution degree was calculated to be 9.4% from ^{1}H nuclear magnetic resonance (^{1}H NMR) spectra (Supporting Information, Figure S6), and could be varied conveniently *via* the feeding ratio of the raw chemicals.

Micelle Formation. The as-prepared PAH-Py methanol solution was diluted with Millipore water to a methanol/water ratio of 1:9 at pH 6.5. The micelles were formed in this solution spontaneously and were kept at 4 °C for dynamic light scattering (DLS) and other characterizations.

1D-NT Formation. The as-prepared PAH-Py methanol solution was diluted with HCl (pH 0) to a methanol/water ratio of 1:9, which was maintained in a vessel under mild agitation for 7 d. The 1D-NTs were formed in this solution and washed with a stirring ultrafiltration cell (Millipore model 8200) to remove the free PAH from the solution. The purified 1D-NT solution was kept at 4 °C for further analyses.

1D-NR Formation. The as-prepared PAH-Py methanol solution was diluted with HCl (pH 2) to a methanol/water ratio of 1:9, which was maintained in a vessel under mild agitation for 2 h. 1D-Nanorods formed in this solution were washed with a stirring ultrafiltration cell to remove the free PAH from the solution. The purified 1D-NR solution was kept at 4 °C for further analyses.

Toluene Extraction Experiment. According to the stoichiometry, there were initially 4.97 mg of Py-CHO and 0.02 g of PAH in 10 mL of PAH-Py solution. After dilution to 100 mL by pH 0 HCl solution or pH 2 HCl solution, respectively, there was 0.0994 mg of Py-CHO in every 2 mL of solution. This 2 mL of PAH-Py solution (pH 0 or pH 2) was transferred to a glass bottle, in which the decomposed Py-CHO was extracted by 2 mL of toluene at the desired time interval during the subsequent process (exactly the same process as that of assembly at pH 0 and pH 2, respectively). The Py-CHO amount in toluene was determined by UV−vis absorption spectroscopy ($\varepsilon_{396} = 1.58 \times 10^4$ M^{-1} cm^{-1}). Data were averaged from 10 parallel experiments, and standard deviation was calculated.

Characterizations. DLS and zeta potential measurements were conducted on a Malvern HPPS 500 and Malvern Zetasizer Nano ZS instrument, respectively. The micellar solution was diluted by 10 times. The NMR spectra were recorded on a Bruker DMX400. TEM images were obtained with a Zeiss EM 912 Omega microscope at an acceleration voltage of 120 kV. SEM measurements were performed with a Gemini Leo 1550 microscope at an acceleration voltage of 3 kV. SFM images were recorded with a Nanoscope IIIa multimode microscope (Digital Instruments Inc., Santa Barbara, CA). Measurements were carried out in tapping mode using silicon tips (Nanosensors, Wetzlar). CLSM images were taken on a LEICA TCS system (Aristoplan, Germany, 100 × oil immersion using commercial software). The samples were prepared by casting the as-prepared solutions of micelles, 1D-NRs, and 1D-NTs onto copper grids with a carbon film (for TEM), silicon wafers (for SEM), newly cleaved mica (for SFM), and glass slides (for CLSM), and air-dried, respectively. Cryo-TEM measurement was performed on a Philips CM12 TEM using the Gatan cryo-holder and -transferstation (model 626, Gatan Inc., USA) at an accelerating voltage of 100 kV. Droplets of the 1D-NT solution (5 μL) were applied to perforated carbon film covered 200 mesh grids, which was deposited with a gold layer to avoid the erosion by the NT solution of low pH. The supernatant fluid was adsorbed with a filter paper until an ultrathin layer of the sample solution was formed, which spanned the holes of the carbon film. The sample was immediately vitrified by propelling the grids into liquid ethane at its freezing point (90 K) operating a guillotine-like plunging device. CD spectra were recorded on a Jasco J-715 spectropolarimeter using a 1 mm rectangular quartz cell. Steady-state fluorescence spectra were measured on a Fluoromax-4 spectrofluorometer (Horiba, Jobin Yvon). XRD measurements were performed on a Bruker D8 Advance diffractometer with Cu Kα1 radiation ($\lambda = 1.5406$ Å). UV−vis spectra were taken by a Cary 4E UV−visible spectrophotometer. FTIR measurements were conducted on a Bruker Equinox 55/S

using a KBr pellet. The polarized optical microscopy images were obtained with an Olympus BX51.

Acknowledgment. We acknowledge C. Böttcher at the Free University of Berlin for Cryo-TEM measurement, A. Eisenberg at McGill University and J.-M. Lehn at Université Louis Pasteur for their valuable discussion and suggestions, and the Max-Planck Society for a visiting grant. This work is financially supported by the Zhejiang Provincial Natural Science Foundation of China (No. Z4090177), the Ministry of Science and Technology of China for the Indo-China Cooperation (No. 2010DFA51510), and the Natural Science Foundation of China (No. 50873087).

Supporting Information Available: Supporting spectroscopy and imaging data. This material is available free of charge *via* the Internet at http://pubs.acs.org.

REFERENCES AND NOTES

1. Yang, L.; Alexandridis, P. Physicochemical Aspects of Drug Delivery and Release from Polymer-Based Colloids. *Curr. Opin. Colloid Interface Sci.* **2000,** *5*, 132–143.
2. Angelatos, A. S.; Katagiri, K.; Caruso, F. Bioinspired Colloidal Systems *via* Layer-by-Layer Assembly. *Soft Matter* **2006,** *2*, 18–23.
3. Sukhorukov, G. B.; Rogach, A. L.; Zebli, B.; Liedl, T.; Skirtach, A. G.; Köhler, K.; Antipov, A. A.; Gaponik, N.; Susha, A. S.; Winterhalter, M.; *et al*. Nanoengineered Polymer Capsules: Tools for Detection, Controlled Delivery, and Site-Specific Manipulation. *Small* **2005,** *1*, 194–200.
4. Vriezema, D. M.; Aragonès, M. C.; Elemans, J. A. A. W.; Cornelissen, J. J. L. M.; Rowan, A. E.; Nolte, R. J. M. Self-Assembled Nanoreactors. *Chem. Rev.* **2005,** *105*, 1445–1489.
5. Shchukin, D. G.; Möhwald, H. Self-Repairing Coatings Containing Active Nanoreservoirs. *Small* **2007,** *3*, 926–943.
6. Van Hest, J. C. M.; Delnoye, D. A. P.; Baars, M. W. P. L.; Van Genderen, M. H. P.; Meijer, E. W. Polystyrene-Dendrimer Amphiphilic Block Copolymers with a Generation-Dependent Aggregation. *Science* **1995,** *268*, 1592–1595.
7. Kishimura, A.; Koide, A.; Osada, K.; Yamasaki, Y.; Kataoka, K. Encapsulation of Myoglobin in PEGylated Polyion Complex Vesicles Made from a Pair of Oppositely Charged Block Ionomers: A Physiologically Available Oxygen Carrier. *Angew. Chem., Int. Ed.* **2007,** *46*, 6085–6088.
8. De Geest, B. G.; Sanders, N. N.; Sukhorukov, G. B.; Demeester, J.; De Smedt, S. C. Release Mechanisms for Polyelectrolyte Capsules. *Chem. Soc. Rev.* **2007,** *36*, 636–649.
9. Li, J. B.; Möhwald, H.; An, Z. H.; Lu, G. Molecular Assembly of Biomimetic Microcapsules. *Soft Matter.* **2005,** *1*, 259–264.
10. Sukhorukov, G. B.; Möhwald, H. Multifunctional Cargo Systems for Biotechnology. *Trends Biotechnol.* **2007,** *25*, 93–98.
11. Wang, Y.; Angelatos, A. S.; Caruso, F. Template Synthesis of Nanostructured Materials *via* Layer-by-Layer Assembly. *Chem. Mater.* **2008,** *20*, 848–858.
12. Basinska, T. Hydrophilic Core-Shell Microspheres: A Suitable Support for Controlled Attachment of Proteins and Biomedical Diagnostics. *Macromol. Biosci.* **2005,** *5*, 1145–1168.
13. Freiberg, S.; Zhu, X. Polymer Microspheres for Controlled Drug Release. *Int. J. Pharm.* **2004,** *282*, 1–18.
14. Daamen, W. F.; Geutjes, P. J.; van Moerkerk, H. T. B.; Nillesen, S. T. M.; Wismans, R. G.; Hafmans, T.; van den Heuvel, L. P. W. J.; Pistorius, A. M. A.; Veerkamp, J. H.; van Hest, J. C. M.; *et al*. "Lyophilisomes": A New Type of (Bio)capsule. *Adv. Mater.* **2007,** *19*, 673–677.
15. Wang, Z. P.; Feng, Z. Q.; Gao, C. Y. Stepwise Assembly of The Same Polyelectrolytes Using Host–Guest Interaction to Obtain Microcapsules with Multiresponsive Properties. *Chem. Mater.* **2008,** *20*, 4194–4199.
16. Antipov, A. A.; Sukhorukov, G. B.; Leporatti, S.; Radtchenko, I. L.; Donath, E.; Möhwald, H. Polyelectrolyte Multilayer Capsule Permeability Control. *Colloid Surf. A, Physicochem. Eng. Asp.* **2002,** *198*, 535–541.
17. Köhler, K.; Sukhorukov, G. B. Heat Treatment of Polyelectrolyte Multilayer Capsules: A Versatile Method for Encapsulation. *Adv. Funct. Mater.* **2007,** *17*, 2053–2061.
18. Skirtach, A. G.; Karageorgiev, P.; Bedard, M. F.; Sukhorukov, G. B.; Möhwald, H. Reversibly Permeable Nanomembranes of Polymeric Microcapsules. *J. Am. Chem. Soc.* **2008,** *130*, 11572–11573.
19. De Geest, B. G.; McShane, M. J.; Demeester, J.; De Smedt, S. C.; Hennink, W. E. Microcapsules Ejecting Nanosized Species into the Environment. *J. Am. Chem. Soc.* **2008,** *130*, 14480–14482.
20. Wang, J.; Xiao, Q.; Zhou, H.; Sun, P.; Yuan, Z.; Li, B.; Ding, D.; Shi, A.; Chen, T. Budded, Mesoporous Silica Hollow Spheres: Hierarchical Structure Controlled by Kinetic Self-Assembly. *Adv. Mater.* **2006,** *18*, 3284–3288.
21. Yu, K.; Zhang, L.; Eisenberg, A. Novel Morphologies of "Crew-Cut" Aggregates of Amphiphilic Diblock Copolymers in Dilute Solution. *Langmuir* **1996,** *12*, 5980–5984.
22. Tung, P. H.; Kuo, S. W.; Chan, S. C.; Hsu, C. H.; Wang, C. F.; Chang, F. C. Micellization and the Surface Hydrophobicity of Amphiphilic Poly(vinylphenol)-*block*-Polystyrene Block Copolymers. *Macromol. Chem. Phys.* **2007,** *208*, 1823–1831.
23. Sha, K.; Li, D.; Li, Y.; Zhang, B.; Wang, J. The Chemoenzymatic Synthesis of a Novel CBABC-Type Pentablock Copolymer and Its Self-Assembled "Crew-Cut" Aggregation. *Macromolecules* **2008,** *41*, 361–371.
24. Menger, F. M.; Seredyuk, V. A. Internally Catalyzed Separation of Adhered Lipid Membranes. *J. Am. Chem. Soc.* **2003,** *125*, 11800–11801.
25. Zhou, Y.; Yan, D. Real-Time Membrane Fission of Giant Polymer Vesicles. *Angew. Chem., Int. Ed.* **2005,** *44*, 3223–3226.
26. Zhou, Y.; Yan, D. Real-Time Membrane Fusion of Giant PolymerVesicles. *J. Am. Chem. Soc.* **2005,** *127*, 10468–10469.
27. Sadasivan, S.; Köhler, K.; Sukhorukov, G. B. Fabrication of Organized Porphyrin-Nanotube-Attached Heat-Senstive Polyelectrolyte Capsules. *Adv. Funct. Mater.* **2006,** *16*, 2083–2088.
28. Wang, Z. P.; Möhwald, H.; Gao, C. Y. Preparation and Redox-Controlled Reversible Response of Ferrocene-Modified Poly(allylamine hydrochloride) Microcapsules. *Langmuir* **2011,** *27*, 1286–1291.
29. Wang, Y.; Bansal, V.; Zelikin, A. N.; Caruso, F. Templated Synthesis of Single-Component Polymer Capsules and Their Application in Drug Delivery. *Nano Lett.* **2008,** *8*, 1741–1745.
30. Tong, W. J.; Dong, W. F.; Gao, C. Y.; Möhwald, H. Charge-Controlled Permeability of Polyelectrolyte Microcapsules. *J. Phys. Chem. B* **2005,** *109*, 13159.
31. Kalyanasundaram, K.; Thomas, J. K. Solvent-Dependent Fluorescence of Pyrene-3-Carboxaldehyde and Its Applications in the Estimation of Polarity at Micelle–Water Interfaces. *J. Phys. Chem.* **1977,** *81*, 2176–2180.
32. Kimura, M.; Miki, N.; Suzuki, D.; Adachi, N.; Tatewaki, Y.; Shirai, H. Wrapping of Self-Organized Fluorescent Nanofibers with a Silica Wall. *Langmuir* **2009,** *25*, 776–780.
33. Matsuzaki, S. Y.; Goto, M.; Honda, K.; Kojima, I. Crystal and Molecular Structures of 1-Pyrenecarbaldehyde. *Anal. Sci.* **1995,** *11*, 461–463.
34. Xiao, J.; Xu, J.; Cui, S.; Liu, H.; Wang, S.; Li, Y. Supramolecular Helix of an Amphiphilic Pyrene Derivative Induced by Chiral Tryptophan through Electrostatic Interactions. *Org. Lett.* **2008,** *10*, 645–648.
35. Balakrishnan, K.; Datar, A.; Oitker, R.; Chen, H.; Zuo, J.; Zang, L. Nanobelt Self-Assembly from an Organic n-Type Semiconductor: Propoxyethyl-PTCDI. *J. Am. Chem. Soc.* **2005,** *127*, 10496–10497.
36. Cordes, E. H.; Jencks, W. P. The Mechanism of Hydrolysis of Schiff Base Derived from Aliphatic Amines. *J. Am. Chem. Soc.* **1963,** *85*, 2843–2848.
37. Schanze, K. S.; Shelton, A. H. Functional Polyelectrolytes. *Langmuir* **2009,** *25*, 13698–13702.